Thus, in choosing surfactants that can make a surface hydrophilic (in contrast to surfactants that simply increase the wettability of the rock by oil), special attention should be paid to the magnitude of the diffusion coefficient of the active substance.

LITERATURE CITED

1. A. Ban, A. F. Bogomolova, et al., Effect of the Properties of Rocks on the Motion of Liquids in Them [in Russian], Gostoptekhizdat, Moscow (1962).
2. P. Ya. Kochina (ed.), Development of Research on the Theory of Percolation in the USSR 1917-1969, Nauka, Moscow (1969).
3. G. I. Barenblatt, V. M. Entov, and V. M. Ryzhik, Theory of Nonstationary Fluid and Gas Percolation [in Russian], Nedra, Moscow (1972).
4. G. A. Babalyan, Physicochemical Processes in Recovering Oil [in Russian], Nedra, Moscow (1974).
5. Sh. K. Gimatudinov, Oil Recovery from Reservoirs [in Russian], Nedra, Moscow (1970).
6. V. M. Entov and N. Shyganakov, "Counterflow capillary permeation of a porous medium by a solution of an active admixture under nonisothermal conditions," Dokl. Akad. Nauk SSSR, 246, No. 4 (1979).

DOUBLE EXPLOSION IN A PERFECT GAS

E. I. Andriankin and N. N. Myagkov

UDC 539.1

Strong-explosion problems have now been examined in some detail. An analytic solution has been obtained [1], the self-modeling equations have been examined [1-3] and approximate and numerical methods have been developed [3-10]. It is of interest to apply a similar process to a double explosion which can be formulated as follows in the simplest case. At time $t = -t_0$ there is an instantaneous release of energy E_1^0 on a plane, on a line, or at a point (symmetry parameter ν respectively 1, 2, and 3). At time $t = 0$, there is a second explosion of energy E_2^0 at the center of symmetry of the first explosion. We assume that the adiabatic parameters γ behind the two explosion-wave fronts are identical, while the density ρ_0 of the unperturbed gas is constant. The first wave is considered as strong. It is obvious that a self-modeling solution [1] applies to the flow between the two fronts before they fuse ($t \leqslant t_c$) and at a large time after fusion ($t \gg t_c$). The non-self-modeling flow behind the second shock wave can be described by numerical methods [4-6, 8-10]. Here we neglect the effects of dissipation, ionization, and radiation emission on the strong explosion. In spite of the simplicity of the formation, the problem is important to explosion theory, since there are two new control parameters $\lambda = E_2^0/E_1^0$ and t_0 by comparison with the classical solution.

After the second explosion and before the fusion ($t \leqslant t_c$), the flow in the region between the fronts is characterized by E_1^0, ρ_0, γ, ν, r, t and therefore is dependent on the single dimensionless variable $\eta = r[E_1 t^2/\rho_0]^{-1}/(\nu+2)$. To describe the flow behind the second front, it is necessary to have the parameters E_2^0 and t_0, because here the flow ceases to be self-modeling and is dependent on the two independent variables η and $\tau = t/t_0$, as well as on the parameters λ^0, ν, γ. Therefore, the calculation must be performed for each particular λ^0, while t_0 is considered as the time scale, by analogy with an explosion with counterpressure. We consider finite $t_0 < \infty$. In that case, the second wave always catches up with the first, since the latter is always strong and any C_+ characteristic catches up with the front in a finite time. The occurrence of a double configuration of waves that do not fuse in practice is related to the counter pressure in the unperturbed gas, which results in a negative phase behind the first wave.

The subscripts $1*$ and $2*$ denote the quantities at the fronts of the first and second shock waves respectively. Subscript * denotes quantities at the front of the wave formed by fusion in the double explosion (resultant wave).

1. Self-Modeling Stages. During the initial instants ($t \ll t_0$) after the second point

Moscow. Translated from Zhurnal Prikladnoi Mekhaniki i Tekhnicheskoi Fiziki, No. 4, pp. 119-125, July-August, 1981. Original article submitted June 4, 1980.

0021-8944/81/2204-0545$07.50

explosion, the shock wave shows self-modeling propagation, since a point explosion is always strong in the initial stage, and therefore the flow is determined by the energy E_2^0 and the power law density distribution at the center of the first explosion at t = 0 (we neglect the pressure and the velocity ahead of the second shock wave front in this approximation), i.e., for times $t \ll t_0$ the first wave is considered as immobile (the successive approximations in which this assumption is correct are considered below). We take the first term in the expansion from the asyptotic representation of the density at the center of the first wave [1]:

$$\rho = Ar^{\omega}, \quad \omega = \nu/(\gamma - 1), \quad E_1^0 = \alpha_1(\nu, \gamma) E_1,$$
$$A = b(\nu, \gamma)\rho_{1*}(r_1^0)^{-\omega}, \quad r_1^0 = r_{1*}(t = 0) = (E_1 t_0^2/\rho_0)^{1/(\nu+2)},$$

where b and α_1 are self-modeling constants and r_1^0 is the position of the front of the first wave at the time of the second explosion (distance scale).

The flow behind the front of the second wave for $t \ll t_0$ is dependent on the self-modeling variable $\xi = r/(r_1^0 x)$, where the quantity $x = r_{2*}/r_{1*}$ is given in this limiting case by the formula

$$x = \frac{r_{2*}}{r_{1*}} = \left[\frac{(\gamma - 1)\lambda\tau^2}{(\gamma + 1) b(\nu, \gamma)}\right]^{\frac{1}{\nu+2+\omega}},$$

where $\lambda = k(\nu, \gamma)\lambda^0$; $\tau = t/t_0$.

The energy balance was used to calculate the values of the self-modeling constant $k(\nu, \gamma)$ for $\gamma = 1.4$ and $\nu = 3$ and 1, the results being respectively 7.42 and 3.84. A solution has been obtained [1, 3] for a strong explosion in a medium or variable density. The late stage corresponding to $t \gg t_c$ is also self-modeling and is described the the solution with energy $E^0 = E_1^0 + E_2^0$ everywhere apart from the central region, where the entropy distribution is dependent on the passage of the two shock waves and the interaction between them. For $t \gg t_c$ the effects of t_0 become negligible and for $\tau \to \infty$ we have

$$p_*/p_{1*} = (1 + \lambda^0)^{2/(\nu+2)}, \quad r_*/r_{1*} = (1 + \lambda^0)^{1/(\nu+2)}. \tag{1.1}$$

The criterion for a self-modeling state after fusion may be taken as a numerical difference, e.g., 5%, of the pressure at the front of the double explosion $p_*(\tau)$ relative to the amplitude $p_0(\tau)$ of the strong explosion of energy E^0, and then the time τ^0 at which this condition is met is defined by

$$[p_*(\tau^0) - p^0(\tau^0)]/p^0(\tau^0) \leqslant 0{,}05. \tag{1.2}$$

Calculations show that the self-modeling stage is reached earlier (i.e., as a smaller τ_0) if τ_c is small, and the resultant wave according to (1.2) will be close to the self-modeling state rather earlier, since the sequences of additional shock waves (see below) formed after the interaction of the waves will catch up with the resultant wave and will violate (1.2). However, with the 5% criterion above, this violation will occur only for the first secondary wave, which is the strongest, and then only for $\lambda^0 \sim 1$, and in order to incorporate the subsequent secondary waves it would be necessary to strengthen (1.2) considerably. The first entry to the self-modeling state occurs in a time comparable with τ_c for a given λ. For example, $\lambda^0 = 5$ $\tau^0 = 3.4\tau_c$, in the planar case for $\lambda^0 = 5$, and $\tau^0 = 2.7\tau_c$ for $\lambda^0 = 1$. The additional shock wave are negligible small for $\lambda^0 \gg 1$ or $\lambda^0 \ll 1$, and therefore the resultant wave goes over to the self-modeling state once, the time required being $\tau^0 \sim \tau_c$. The second entry to the self-modelling state for $\lambda^0 \sim 1$ occurs for the τ^0 considerably exceeding the τ_c corresponding to this λ^0, but here again τ^0 increases monotonically with τ_c.

2. First and Second Approximations for the Second Explosion for $\tau \ll 1$. In considering the self-modeling behavior of the second explosion for $\tau \ll 1$ we assumed that the first wave was immobile ($r_{1*} = r_1^0$).

We consider the first approximations following the self-modeling one in relation not only to the density but also the the pressure and velocity ahead of the second wave front. The approximation is performed in terms of the time variable $x = r_{2*}/r_{1*}$, basically following the method surveyed in [3]. The medium ahead of the second front corresponds to the central

integral in the first shock wave:

$$\rho = b(\nu, \gamma)\rho_{1*}(r/r_{1*})^{\omega}, \quad p = h_1(\nu, \gamma)p_{1*}, \quad v = \sigma(\nu, \gamma)xv_{1*}. \tag{2.1}$$

The equations of gas dynamics for the second wave are taken in divergent form and transformed to the variables

$$g = \rho/\rho_{2*}, \quad h = p/p_{2*}, \quad \varphi = (r_{2*}v)/(D_{2*}r),$$
$$\xi = r^{\nu}/r_{2*}^{\nu}, \quad x = r_{2*}/r_{1*}. \tag{2.2}$$

We represent the approximate solution around the point x = 0 as an asymptotic series in x^{ν}:

$$\mathbf{G} = \sum_i \mathbf{G}^{(i)}x^{\nu i}, \quad i = 0, 1, 2, \ldots, \tag{2.3}$$

where G is a column vector with components g, h, e, φ, where

$$e = h + \left(\frac{\gamma+1}{2}\xi^{1/\nu}\varphi\right)^2 g.$$

The following is the approximation for the front speed [2]:

$$-\ln D^2 = \ln(A_0x^{\omega+\nu}) + A_{10}x^{\nu} + A_{20}x^{2\nu} + \ldots,$$
$$D = D_{2*}/D_{1*}, \quad A_0 = [(\nu+2+\omega)^2 b(\nu, \gamma)(\gamma+1)]/[(\nu+2)^2\lambda(\gamma-1)],$$

where A_{10} and A_{20} are unknown constants to be determined. The following are the boundary conditions at the front (ξ = 1) of the second wave:

$$g_{2*}^{(0)} = 1, \quad h_{2*}^{(0)} = 1, \quad \varphi_{2*}^{(0)} = 2/(\gamma+1), \quad g_{2*}^{(i)} = 0, \quad h_{2*}^{(i)} = 0, \quad i = 1, 2,$$
$$\varphi_{2*}^{(1)} = -4\gamma H(\nu, \gamma, \lambda)/(\gamma^2-1), \quad H = \left(\frac{\gamma-1}{\gamma+1}\right)^2 \frac{h_1A_0}{b(\nu, \gamma)}, \tag{2.4}$$

where h_1 is the counterpressure ahead of the second wave of (2.1). At the center ξ = 0 we have

$$\varphi(0, x) = 1/\gamma + x^{\nu}\varphi^{(1)}(0) + x^{2\nu}\varphi^{(2)}(0) + \ldots,$$

where the $\varphi_0^{(i)}$ are constants. We substitute the expansion of (2.3) into the initial system of equations as transformed to the variables of (2.2) and arrange the terms $x^{\nu i}$ with identical i = 0, 1, 2 to get systems of ordinary differential equations for the corresponding approximations.

The value i = 0 corresponds to a self-modeling solution for a strong explosion in the medium of variable density. The second wave remains self-modeling with high accuracy for x not very small, the exact value being determined by λ. For example, in the spherical case we have x = 0.11 for λ^0 = 1, and for λ^0 = 10 we have 0.25, and the pressure at the front of the second wave exceeds the pressure ahead of the front by approximately a factor 100.

We consider the first approximation (i = 1). We assume that ω > ν − 2 in order to neglect terms of higher order in (2.1) in the expression for the density expansion in the central interval of the first wave.

The following in the system of equations for the first approximation:

$$g^{(1)}\left(\frac{\omega}{\nu}+1\right) - \frac{4\gamma}{(\gamma-1)^2}Hg^{(0)} - \xi g^{(1)\prime} + [\xi(g^{(0)}\varphi^{(1)} + g^{(1)}\varphi^{(0)})]' = 0,$$
$$-(A_{10}+H)e^{(0)} - \xi e^{(1)\prime} + [\xi\varphi^{(0)}(e^{(1)} + (\gamma-1)h^{(1)}) + \xi\varphi^{(1)}(e^{(0)} +$$
$$+ (\gamma-1)h^{(0)}]' = 0,$$
$$-(A_{10}+H)h^{(0)} - \xi h^{(1)\prime} + \gamma(\varphi^{(0)}h^{(1)} + \varphi^{(1)}h^{(0)}) +$$
$$+ \xi(\varphi^{(0)}h^{(1)\prime} + \varphi^{(1)}h^{(0)\prime}) + \gamma\xi(h^{(0)}\varphi^{(1)\prime} + h^{(1)}\varphi^{(0)\prime}) = 0,$$
$$e^{(1)} = h^{(1)} + \left(\frac{\gamma+1}{2}\xi^{1/\nu}\right)^2(\varphi^{(0)2}g^{(1)} + 2\varphi^{(0)}\varphi^{(1)}g^{(0)}) \tag{2.5}$$

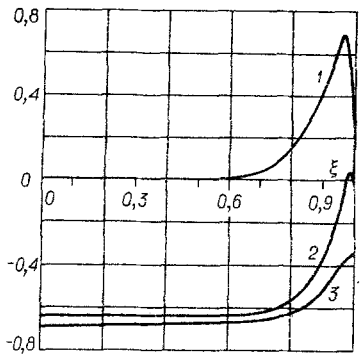

Fig. 1

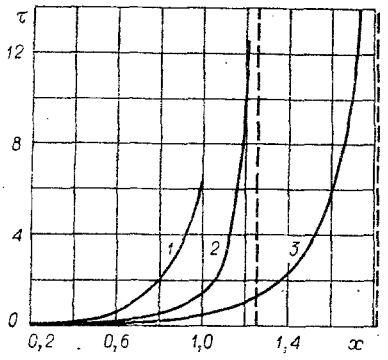

Fig. 2

(primes denote derivatives with respect to the variable ξ).

System (2.5) contains the constants A_{10}. We split the dependent variables $G^{(1)} = G^{(11)} + A_{10}G^{(12)}$ into two systems of equations for $G^{(11)}$ and $G^{(12)}$ and combine these with the self-modeling equations for $G^{(0)}$ and the boundary conditions of (2.4) to get a closed system of equations for numerical solution for the first approximation. This system has an integral analogous to that given in [3] (p. 122). The parameter $H \sim 1/\lambda$ appears linearly in (2.5) and in the corresponding boundary conditions of (2.4), i.e., division of all the equations by H results in a system independent of λ. This important property enables one to derive the numerical solution for some one λ°, for example $\lambda^\circ = 1$. The solutions for other λ° were obtained by simple division by λ° (for given ν and γ).

Consequently, in the first approximation we can write for the dependent variables that

$$G = G^{(0)} + (x^\nu/\lambda)Q^{(1)},$$

where $Q^{(1)} = G^{(1)}\lambda$ is not dependent on λ. In this approximation, λ appears in G only in the combination $T = x^\nu/\lambda$ (time scale). Figure 1 gives a numerical solution in the first approximation for the planar case, $\gamma = 1.4$, $\nu = 1$; curve 1 denotes the density $g^{(2)}$, 2 the pressure $h^{(1)}$, and 3 the velocity $\varphi'^{(1)}$.

In the second approximation, the density in the central interval of the first wave is taken in the form of (2.1), and it is therefore necessary to put $\gamma < 1 + \nu/(2\nu - 2)$; in the equations for this approximation, the boundary conditions for the front introduce the counterpressure h_1 and terms proportional to x^β ($\beta = (\omega + \nu + 2)/2$), which incorporate the motion of the medium ahead of the second front and the motion of the first front. For $\gamma < 1 + \nu/(3\nu - 2)$ we always have $\beta > 2\nu$, and the first wave can be considered as immobile, as in the first approximation. In that case the second approximation may be considered by analogy with the first, and the distortion due to the motion of the first wave appears only in the third approximation.

For λ small, the scale x^ν/λ characterizes the presence of a singularity of boundary-layer type at the center, at which there are sharp changes in the quantities at the second front. This singularity occurs in a double explosion (in contrast to the self-modeling solution for the single explosion) due to the presence of the characteristic scale r_1^0 (or t_0). The following estimates may be made from the first approximation: $x^\nu \ll \lambda$ is the region where the second explosion is strong, and $\lambda \ll x^\nu \leqslant 1$ is the region where the second shock wave degenerates into a quasiacoustic one (for $\lambda \ll 1$).

The first approximation was used here to supply the initial data for the numerical solution.

3. Numerical Results. The limiting cases $\tau \ll 1$ and $\tau \gg 1$ correspond to self-modeling solutions. The problem has been solved numerically for a wide range of times for intermediate values of τ.

The solution was obtained by Godunov's method with explicit and inexplicit schemes, which are described in [6].

The second front was identified during the computation, as well as the resultant front

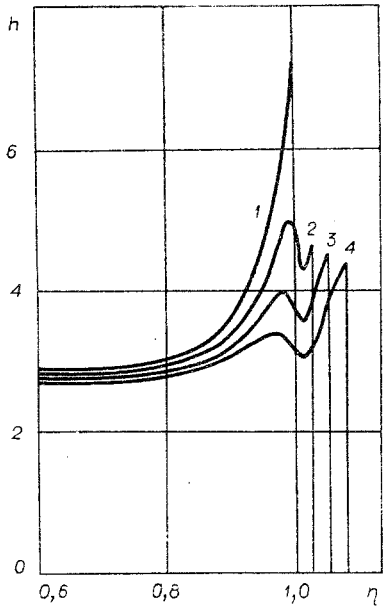

Fig. 3

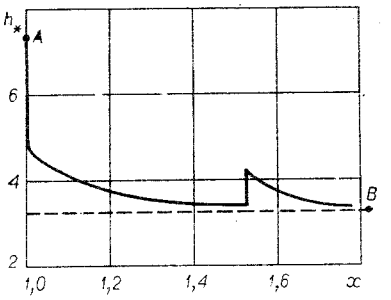

Fig. 4

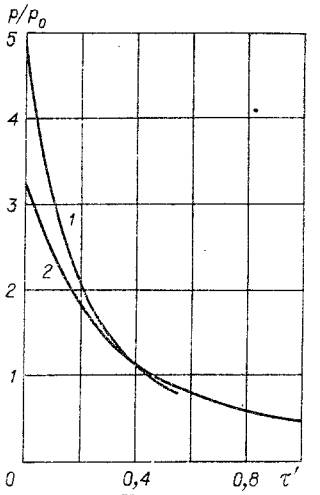

Fig. 5

after fusion. The error in the calculation was checked from the conservation of mass and energy over the entire flow field. The errors were not more than 2-4%. For $\tau < \tau_c$, the flow ahead of the second front was calculated at each step from the self-modeling equations for the strong explosion. For $\tau \geqslant \tau_c$, the initial approximation for the pressure in the algorithm for the decay of the discontinuity at the resultant front was specified as the pressure at the front of the self-modeling wave corresponding to the overall energy of the two waves. The numerical solutions were derived for $\lambda^\circ = 1$ and 5 for $\gamma = 1.4$ in the planar case ($\nu = 1$). Figures 2-5 give the numerical results.

Dimensional considerations indicate that the time is related to the position of some one of the fronts $x = r_*/r_{1*}$ by $\tau = \tau(\gamma, \nu, \lambda, x)$, which is shown in Fig. 2. The straight line $x = 1$ corresponds to the path of the first shock wave. Curve 1 in Fig. 2 is for $\lambda^\circ = 0$ (C_+ characteristic), while 2 is for $\lambda^\circ = 1$ and 3 for $\lambda^\circ = 5$. All the fusion times fall in the range from 0 to τ_+ (τ_+ is the time for the first wave to reach the C_+ characteristic). For $\nu = 1$ and $\gamma = 1.4$ the calculations gave the following values: $\tau_+ = 6.41$, $\tau_c(\lambda^\circ = 1) = 1.406$, $\tau_c(\lambda^\circ = 5) = 0.515$. The self-modeling state is attained for $\tau \to \infty$ in Fig. 2 and is expressed as curves 2 and 3 tending asymptotically to the broken straight line, the equations for these being derived from (1.1) by substituting $\lambda^\circ = 1$ and 5.

When the two waves fuse, an unstable configuration is formed at $x = 1$, which breaks up at the next instant into the resultant shock wave and an expansion wave traveling towards the symmetry plane. Figure 3 shows the evolution of the discontinuity for a certain time after

the fusion for $\lambda^\circ = 5$, with the symbols corresponding to the following instants: 1) $\tau \approx 0.515$, 2) $\tau \approx 0.571$, 3) $\tau \approx 0.631$, 4) $\tau \approx 0.69$. After the decomposition, the pressure at the first C_- characteristic of the decompression wave exceeds the pressure at the front of the resultant shock wave for a time $\Delta\tau$ (0.066 for $\lambda^\circ = 1$ and 0.077 for $\lambda^\circ = 5$). The ordinate in Fig. 3 is the pressure $h = p/p_{1*}$, while the abscissa is the variable $\eta = r/r_{1*}$.

In this coordinate system, the resultant wave tends to an immobile (self-modeling) profile for $\tau \to \infty$ with the pressure at the front from (1.1).

Figure 4 shows the pressure envelope for the resultant front from the time of fusion (point A with coordinates $x = 1$, $h_* = 7.365$) for $\lambda^\circ = 5$. The calculation for this case was carried through to $x = 1.78$, which corresponds to $\tau = 25.7$. The limiting point B to which the pressure at the front tends for $\tau \to \infty$ has the coordinates of (1.1). Figure 4 shows the discontinuous character of the numerical solution in the self-modeling state. Here we show the fusion of the first and strongest of the additional shock waves with the front of the resultant wave, these additional waves arising from reflection of the decompression wave from the high-entropy zone near the center [11]. The first of these additional shocks corresponds to reflection of the strongest decompression wave from the high-entropy zone, this being formed at $x = 1$ (Fig. 3). The additional shock waves become diffuse during the calculation, so the step in Fig. 4 has been constructed by means of a special procedure analogous to that used in [12].

It is of interest to compare the reflection from an undeformable wall for the waves in the double explosion and the self-modeling wave with the same total energy. Figure 5 shows the dependence of the pressure p/p_0 ($p_0 = \rho_0(r_1^0/t_0)^2$ is the pressure scale) at the wall as a function of time τ' from the start of reflection for $\lambda^\circ = 1$, with the wall placed in the plane $x = 1$ of front fusion for the double explosion. At the instant of collision with the wall ($\tau' = 0$), the pressure from the double explosion considerably exceeds that from a self-modeling shock wave. Then curve 1 (reflection of the double explosion) and 2 (reflection of the self-modeling shock wave) fall rapidly and attain identical pressures in time $\tau'_* = t_*/t_0 = 0.39$. During this time, the dimensionless pressure impulse $I/I_0 = \int_0^{\tau_*} p/p_0 d\tau'$ in the reflected shock wave from the double explosion exceeds the impulse from the self-modeling wave by $\Delta I/I_0 \approx 0.13$, which constitutes about 14% of I/I_0 for the double explosion.

Here the characteristic scale of the process is t_0. Consideration of the dimensions shows that ΔI increases with t_0 as $\Delta I \sim t_0^{1/3}$ for given γ and ν. The increase in ΔI from t_0 is bounded, of course, by the applicability of the strong-explosion approximation for each particular case.

In the same way the above method can be used to consider a double explosion in a medium with an initial variable density distribution, and one can also consider the counter pressure and the effects of thermal conductivity. Allowance for ionization and dissociation alters the equation of state for the perturbed medium, although this can be described approximately by introducing, for example, an effective adiabatic parameter. The radiative transport produces a zone of finite density and temperature near the center of a double explosion [13, 14], and in the late stages results in detachment of the burned sphere from the shock wave [15].

LITERATURE CITED

1. L. I. Sedov, Similarity and Dimensions Methods in Mechanics [in Russian], 8th edition, Nauka, Moscow (1977).
2. K. P. Stanyukovich, Transient-State Motion of a Continuous Medium [in Russian], Nauka, Moscow (1971).
3. V. P. Korobeinikov, N. S. Mel'nikova, and E. V. Ryazanov, Theory of Point Explosions [in Russian], Fizmatgiz, Moscow (1961).
4. Kh. S. Kestenboim, G. S. Rozlyakov, and L. A. Chudov, Point Explosions [in Russian], Nauka, Moscow (1974).
5. S. K. Godunov, A. V. Zabrodin, et al., Numerical Solution of Multidimensional Problems in Gas Dynamics [in Russian], Nauka, Moscow (1976).
6. H. Broude, Explosion Calculation by Computer [Russian translation], Mir, Moscow (1976).
7. G. G. Chernyi, "Adiabatic motion of a perfect gas in a high-intensity shock wave," Izv. Akad. Nauk SSSR, OTN, No. 3 (1957).

8. D. E. Okhitsimskii, I. L. Kondrasheva, et al., "Calculation of a point explosion with allowance for counter pressure," Trudy MIAN SSSR, 50, 1 (1957).
9. V. P. Korobeinikov and P. I. Chushkin, "Method of calculating a point explosion in a gas," Dokl. Akad. Nauk SSSR, 154, No. 3 (1964).
10. V. P. Korobienikov and L. V. Shidlovskaya, "A numerical solution for an explosion in a moving gas," in: Numerical Methods in the Mechanics of Continuous Media [in Russian], Vol. 6, No. 4 (1975).
11. E. I. Andriankin, "High-Speed collision of two plates," Zh. Prikl. Mekh. Tekh. Fiz., No. 4 (1963).
12. V. V. Podlubnyi and A. S. Fonarev, "Reflection of a spherical wave from a flat surface," Izv. Akad. Nauk SSSR, Mekh. Zhid. Gaza, No. 6 (1974).
13. É. I. Andriankin, "Effects of radiative conduction on the gas flow in a strong explosion," Inzh.-Fiz. Zh., 4, No. 11 (1961).
14. É. I. Andriankin, "Propagation of a non-selfmodeling heat wave," Zh. Eksp. Teor. Fiz., 35, No. 2 (8) (1958).
15. Ya. B. Zel'dovich and Yu. P. Raizer, Physics of Shock Waves and High-Temperature Hydrodynamic Phenomena [in Russian], Fizmatgiz, Moscow (1963).

INVESTIGATION OF THE SHOCK COMPRESSION OF LIQUID TIN AT PRESSURES UP TO 100 GPa AND INITIAL TEMPERATURES OF 310...475°C

K. V. Volkov and V. A. Sibilev

UDC 536.242:546.3

The melting of materials when subjected to shock compression and the equation of state of the liquid phase has been considered in [1-4]. Numerous experimental results on the dynamic compressibility of different materials up to 1 TPa, e.g., [5-7], show that melting in a shock wave is only slightly affected by the variation of the shock adiabatic curve in p–U and p–V coordinates (p is the pressure, U is the mass velocity, and V is the specific volume). The experimental data up to pressures of 0.1-0.15 TPa are well described by a linear D–U relationship. At higher pressures there is a reduction in the slope of the D–U curve, due to melting in the shock wave [3], and the D–U curve in the liquid-phase region takes the form of a straight line but with a smaller slope than for the solid phase. However, it should be noted that from the existing experimental points one could equally successfully draw a D–U curve with a gradually reducing slope. Such attempts have been made (see, e.g., [8]). On the other hand, it was pointed out in [3] that a gradual reduction in the slope of the D–U curve may be due to an increase in the contribution of the electron component in the equation of state at high temperatures. Hence, it is difficult to draw any definite conclusions regarding the effect of melting on the form of the D–U curve. Information on this can, in principle, be obtained if one has experimental D–U curves of the initially solid and initially liquid phases. We know of only one publication in which shock compression of a liquid metal (mercury) has been investigated [9]. As far as we are aware no comparative data on the shock loading of an initially liquid and an initially solid phase of metals exists.

1. Calculation of the Shock Adiabatic Curves of Al and Cu and an Estimate of the Shock Adiabatic Curves of Liquid Sn. Using the semi-empirical equations of state proposed in [3] we calculated the shock adiabatic curves of the initially solid and liquid phases of Al and Cu. The initial state of the liquid phases was taken at t = 2000°C for Al ($\rho_{0l} \approx 2.1$ g/cm^3, and $E_{0l} \approx 217 \cdot 10^8$ erg/g) and at t = 2500°C for Cu ($\rho_{0l} \approx 7.1$ g/cm^3 and $E_{0l} \approx 142 \cdot 10^8$ erg/g). Considerable overheating above the melting point was then taken in order to explain the difference in the behavior of the shock adiabatic curves of the solid and liquid phases and particularly the slope of the D–U curves. We also carried out calculations using the equation of state of the liquid phase for the initially solid state of Al and Cu (Table 1).

In Fig. 1 (in the same coordinates as in [3]) we plot curves for Al (curve 1 is experimental [10], curve 2 is calculated for the solid phase, curve 3 is calculated for the liquid phase with ρ_{0l}, E_{0l}, curve 4 is calculated for the liquid phase with ρ_{0s}, E_{0s}, and curve 5 is

Translated from Zhurnal Prikladnoi Mekhaniki i Tekhnicheskoi Fiziki, No. 4, pp. 125-132, July-August, 1981. Original article submitted June 4, 1980.

0021-8944/81/2204-0551$07.50